

What do we really know about the low-ionization structures in planetary nebulae?

Stavros Akras

Institute for Astronomy, Astrophysics, Space Applications and Remote Sensing, National Observatory of Athens, GR 15236 Penteli, Greece
email: stavrosakras@gmail.com

Abstract. We do know that planetary nebulae (PNe) are ionized gaseous clouds of material ejected by evolved dying stars. The intense ultraviolet radiation field of these stars leads to the dissociation of the cold molecular gas and then to the ionization/excitation of the resultant atomic gas. The chemical composition, ionization structure, physical conditions and formation process of nebular shells, rims, and halos are well comprehended. On the contrary, the origin of low-ionization structures (LISs) frequently found in PNe break the overall picture, and it still remains poorly understood. The latest discoveries of molecular hydrogen (H_2) in LISs have changed how we think about their origin. Besides the detection of H_2 emission, the [Fe II] $1.644\mu m$ and [C I] 8727\AA lines have also been detected in LISs. These results add new pieces to the puzzling problem of LISs opening a new window to enrich our knowledge and understanding on these microstructures.

Keywords. (ISM:) planetary nebulae: general, ISM: atoms, ISM: molecules, planetary nebulae, (ISM:) dust, extinction

1. Introduction

Planetary nebulae (PNe) are complex batches of expanding and interacting shells of gas and dust expelled from low-to-intermediate mass stars ($1-8 M_\odot$), during the active red-giant (RG) and asymptotic giant branch (AGB) evolutionary stages via stellar winds and pulsations. The gas (ionic, atomic and molecular) forming a PN is the debris of these progenitors stars. The intense UV radiation field of the exposed hot and luminous central star (CS) is the dominant source of highly energetic photons that lead, first, to the dissociation of the cold molecular circumstellar envelope (mainly H_2 , CO) and, then, to the ionization/excitation of the resulting atomic gas causing the nebula to glow ([Kwitter & Henry 2022](#)).

From a morphological point of view, PNe display a number of nebular structures such as rims, shells and halos surrounding the CS, as well as structures in smaller-scales prominent in low-ionization species e.g. [N II], [S II], [O II], [O I] (hereafter LISs; [Gonçalves et al. 2001](#)), and easily discerned from the host nebulae. Moreover, based on their kinematic properties, LISs are also divided into the fast, low-ionization emission regions (FLIERs, [Balick et al. 1993, 1998](#)), the bipolar, rotation episodic jets (BRETs, [López et al. 1995](#)), and the slow moving low ionization emitting regions (SLOWERs, [Perinotto 2000](#)).

Considering the intense UV radiation from the CSs, photo-ionization/excitation processes are innately considered as the predominant mechanism for the observed emission-line spectra of PNe. However, this fails to explain simultaneous the enhanced

emission in LISs and the surrounding shell, indicating significantly different physical conditions. The origin of LISs continues intriguing the scientists. Their formation cannot be explained by the Generalized Interacting Stellar Wind model (GISW, Balick 1987) and additional mechanisms such as (i) collimated jets/outflows (e.g., Balick et al. 2020) and/or (ii) hydrodynamical instabilities (Kelvin-Helmholtz and/or Rayleigh-Taylor) at the ionization and shock fronts (e.g. Steffen & López 2004; Segura et al. 2006) are required to elucidate their origins.

2. Low-ionization structures: the atomic/ionical component

Based on observations in the visible wavelengths (e.g. Akras & Gonçalves 2016; Mari et al. 2023a,b), it has been found that LISs are characterized by (I) systematically lower electron density (N_e) which contradicts the predictions of dense clumps formation models, (II) comparable electron temperatures (T_e) and (III) similar chemical composition relative to the host nebula. LISs also display significantly lower ionization state than the host nebulae, as it has been shown by the $[\text{O I}]/\text{H}\alpha$ vs $[\text{O II}]/[\text{O III}]$ diagnostic diagram (Mari et al. 2023b). Regarding their excitation mechanisms, the comparison of the observations with the predictions from photoionization and shock models indicates that the vast majority of LISs are more likely photo-dominated structures, but shocks cannot fully rule out yet (Mari et al. 2023b). Overall, LISs akin to photodissociated regions (PDRs).

MUSE data of PNe have offered the opportunity to carry out a spectroscopic analysis in both spatial dimensions covering the host nebulae and LISs (e.g. Walsh et al. 2018; Monreal-Ibero & Walsh 2020). An increase in interstellar extinction $c(\text{H}\beta)$ and electron temperature derived from the $[\text{S III}]$ diagnostic lines (T_e) have been found in the LISs of NGC 7009 relative to the host nebula (Walsh et al. 2018; Akras et al. 2022). These findings likely indicates the presence of more dust and the contribution of photoelectric dust heating. Based on emission line diagnostic diagrams, LISs occupy the regime of low-ionization nebulae, and they are well distinguished from the host nebula (Akras et al. 2022).

The spectral range of MUSE (4560Å to 9300Å) may not allow the detection of the $[\text{O III}]$ $\lambda 4363$ line flux and consequently, the estimation of T_e , but we can look for the detection of the far-red $[\text{C I}]$ $\lambda 8727$ line. $[\text{C I}]$ lines are important coolants of gas in PDRs (Burton et al. 1992) and they imply the presence of free carbon and an oxygen/carbon (O/C) zone. Surprisingly, the $[\text{C I}]$ $\lambda 8727$ line is present in LISs of NGC 6778 (García-Rojas et al. 2022), NGC 7009 (Akras et al. in prep.) and NGC 3242 (Konstantinou et al. in prep.).

Moreover, a pilot $[\text{Fe II}]$ 1.644 μm narrowband image survey has been conducted in PNe with LISs [Program ID: GN-2017A-Q-58, PI: S. Akras]. $[\text{Fe II}]$ lines are common tracers of shocks, and they have been detected in different astronomical environments. The preliminary analysis has shown that LISs also emit in the $[\text{Fe II}]$ 1.644 μm line. Figure 1 displays the PN NGC 7009 in the optical (HST, left panel and MUSE, right panel) and near-infrared (Gemini, middle and inner panels). The LISs in this nebula are characterized by the detection of the $[\text{N II}]$, $[\text{C I}]$, H_2 and $[\text{Fe II}]$ emission lines. All these lines are typical for low-ionization environments such as PDRs.

3. Low-ionization structures: the molecular component

Molecular gas concentrated in small clumps/knots or filamentary structures has already been found in the Helix nebula (Speck et al. 2002; Matsuura et al. 2009), NGC 2346 (Manchado et al. 2015) and very recently in NGC 3132 (De Marco et al. 2022) and the Ring nebula (Wesson et al. 2023) with the remarkable data from the James Webb Space Telescope (JWST).

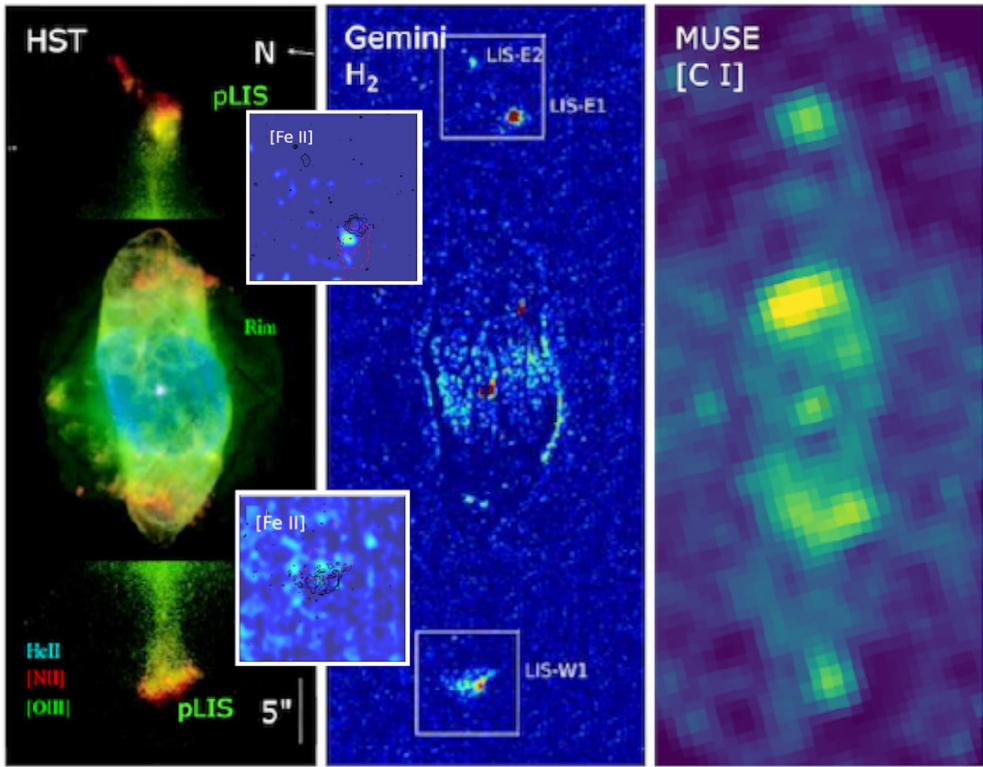


Figure 1. Multi-wavelength picture of the archetypal NGC 7009. Left panel: The optical RGB HST image ([O III] $\lambda 5007$ in green, [N II] $\lambda 6584$ in red and He II $\lambda 4686$ in cyan from Balick et al. (1998). Middle panel: The near-IR continuum-subtracted H₂ $v=1-0$ 2.12 μm Gemini image (Akras et al. 2020). The white squares indicate the two LISs of the nebula. Right panel: The optical MUSE [C I] $\lambda 8727$ emission line map (Akras et al., in prep.). Inner panels: The near-IR continuum-subtracted [Fe II] 1.644 μm Gemini image of the LISs (Akras et al. in prep.). The solid black and dashed red contours indicate the H₂ 1-0 and Br γ emission lines. Both LISs in NGC 7009 are composed of ionic, atomic and molecular gas components.

Gonçalves et al. (2009) suggested that the mass of LISs must be mostly neutral, and, therefore, unobserved in the visible light. The enhanced [O I] $\lambda 6300$ line in LISs was a strong indicator for the presence of an H₂ component (Reay et al. 1988). Recent near-IR observations have unveiled that LISs are also made of molecular gas (Akras et al. 2017; Akras et al. 2020; Fang et al. 2018). Figure 1 shows the continuum-subtracted H₂ 2.12 μm line images of NNG 7009 and Figure 2 presents the optical and continuum-subtracted H₂ images of three new PNe: NGC 6818, NGC 2392, and NGC 7354. [N II] $\lambda 6584$ is found to be co-spatial with H₂ emission line. This reinforces the idea that some LISs, if not all, are made of molecular gas.

Therefore, LISs and H₂ clumps are apparently the two sides of the same coin of (“Dense Molecular Low-Ionization structures” (hereafter DMLISs; see Figure 3). Yet, the origin of H₂ gas still remain an open question. **Are DMLISs fossils of AGB winds surviving for thousands of years, or formed in situ during the PN stage due to shocks and UV radiation?**

The flux ratio of the two brightest molecular hydrogen lines, $R(\text{H}_2) = \text{H}_2 \text{ 2.12 } \mu\text{m} / \text{H}_2 \text{ 2.24 } \mu\text{m}$, is commonly used to disentangle the photo-heated ($R(\text{H}_2) \sim 3$) and shock-heated regions ($R(\text{H}_2) > 10$) (e.g. Marquez-Lugo et al. 2015). However, it is well-known that the UV pumping H₂ emission can also be thermalized in high densities ($10^4\text{--}7 \text{ cm}^{-3}$)

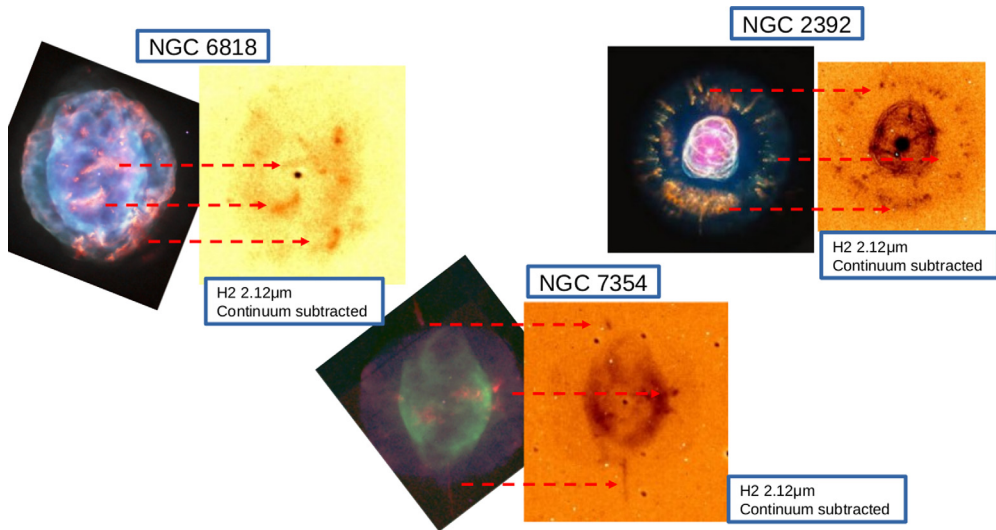


Figure 2. Optical (left panels) and Gemini near-IR (right panels) images of three PNe: NGC 6818, NGC 2392, and NGC 7354. The red arrows indicate the $([\text{N II}])$ and H_2 emission from the same low-ionization structures.

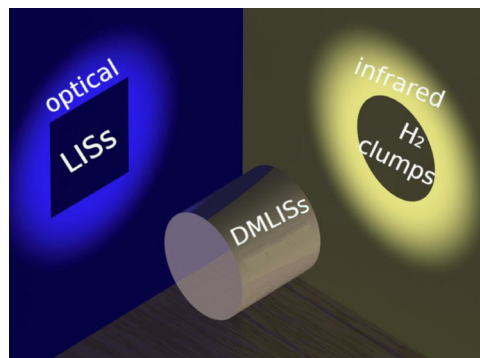


Figure 3. The two sides of the same coin. Low-ionization structures are the DMLISSs in the optical wavelengths and H_2 clumps in the near-Infrared wavelengths.

environments (Sternberg & Dalgarno 1989; Burton et al. 1990), yielding to ratios as high as those of shocks. As a consequence, the $R(\text{H}_2)$ ratio is not an adequate parameter for the determination of the excitation mechanisms in DMLISSs. The observed $R(\text{H}_2)$ values of LISSs have not yet led to a firm conclusion about their excitation mechanism (Akras et al. 2020).

The bombardment of H_2 clumps by highly energetic FUV photons results in the dissociation and photoevaporation of the gas (e.g. Mellema et al. 1998) and consequently in the formation of a photodissociation region (PDR) around the dense H_2 core (see Figure 4 and Speck et al. 2002). An equivalent stratification has also been observed in the LISSs of NGC 7009 (Akras et al. 2022). High-to-moderate ionization lines (He II , $[\text{O III}]$) have their peak intensity closer to the CS than the low-ionization ($[\text{N II}]$, $[\text{S II}]$) ones. The latter lie closer to the CS than the atomic ones ($[\text{O I}]$), which also lie closer to the CS than the H_2 lines. This overall picture of DMLISSs resembles the structure of PDRs (Black & van Dishoeck 1987) and the photoevaporation process can provide a reasonable explanation for the lower N_e measured in the LISSs relative to the surrounding gas and line stratification.

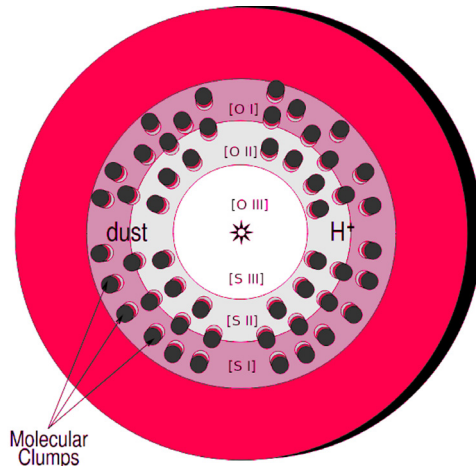


Figure 4. A cartoon of the clumpy envelope in PNe taken from [Speck et al. \(2002\)](#). The ionization stratification is indicated with the O and S emission lines.

PDRs are neutral gaseous regions formed by the penetration of FUV radiation into molecular clouds. A characteristic feature of PDRs is the presence of polycyclic aromatic hydrocarbon (PAH) molecules. PAHs play a crucial role as catalysts in the formation of H_2 via the absorption of H atoms. Despite the detection of PAHs in PNe with Spitzer (e.g. [Perea-Calderón et al. 2020](#)), the low spatial resolution of the data have not allowed the direct association of PAHs with DMLISs yet. A very narrow region at the outer parts of NGC 6720 is found to exhibit an excess in the JWST bands that contain the 3.3 and 11.3 μm PAH features ([Wesson et al. 2023](#)).

4. Dense molecular low-ionization structures: their origin

Despite the intense UV radiation from CS, H_2 molecules can survive, given that the timescale to dissociate them is still larger than the lifetime of PNe (thousands of years). Observations of cool evolved stars have shown that their highly in-homogeneous winds are composed of large amount of dust and molecules, while dense clumps are constantly formed and destroyed ([Weigelt et al. 2002](#); [Ziurys 2006](#); [Ramstedt et al. 2020](#); [Decin 2021](#)) and indicated by 2D hydrodynamic models (e.g. [Woitke 2006](#)). While the photodissociation front is propagated into the circumstellar envelope, it destroys some of these molecular clumps, but not the extremely dense ones, which may survive for thousands of years, and they eventually turn out to be engulfed by the resultant ionized nebular gas ([Graham et al. 1993](#)). As a consequence, DMLISs plausibly represent fossil condensations of the AGB winds which have not been fully dissociated yet, and they are currently being photo-evaporated (see [Redman et al. 2003](#)). On the other hand, dynamic instabilities (e.g. Rayleigh-Taylor, Vishniac or thin-shell instabilities) due to the interaction of the stellar winds or at the ionization-shock front may also lead to the in situ formation of molecular clumps (e.g. [Dyson et al. 2000](#); [Steffen & López 2004](#); [Segura et al. 2006](#)).

Both mechanisms have been proposed to explain the formation of the cometary globules in the Helix nebula. [Matsuura et al. \(2009\)](#) argued that some portion of H_2 gas in the globules is primordial from the AGB phase, whereas [Segura et al. \(2006\)](#) claimed based on hydrodynamical simulations that a portion of the globules may have formed by the dynamic instabilities.

5. Discussion and Conclusions

Low-ionization structures have been studied mainly in the visible wavelength, and only a portion of their true structure has been unveiled. The recent observational attempts in the near-IR have complemented the optical studies and unveiled their true structure as “Dense Molecular Low-Ionization structures”. NGC 7009 serves as the archetypal planetary nebulae for the study of LISs. Besides the typical low-ionization lines [N II], [S II] and [O I], both LISs in NGC 7009 have been detected in the [C I], [Fe II] and H₂ 1-0 lines.

A new window of multi-wavelength study of LISs is now open to get new pieces to the puzzling problem of LISs and valuable insights in their origin and formation mechanisms, as well as explore their possible link with clumps from previous evolutionary stages.

Acknowledgments. The research project is implemented in the framework of H.F.R.I call “Basic research financing (Horizontal support of all Sciences)” under the National Recovery and Resilience Plan “Greece 2.0” funded by the European Union - NextGenerationEU (H.F.R.I. Project Number: 15665).

References

- Akras S., Gonçalves D. R., 2016, *MNRAS*, 455, 930A
 Akras S., Gonçalves D. R., Ramos-Larios G., 2017, *MNRAS*, 465, 1289A
 Akras S., Gonçalves D. R., Ramos-Larios G., Aleman I., 2020, *MNRAS*, 493, 3800A
 Akras S., et al., 2022, *MNRAS*, 512, 2202A
 Balick B., 1987, *AJ*, 94, 671B
 Balick B., Rugers M., Terzian Y., et al., 1993, *ApJ*, 411, 778
 Balick B., Alexander J., Hajian A. R., et al., 1998, *AJ*, 116, 360B
 Balick B., et al., 2020, *ApJ*, 889, 13
 Black J. H., van Dishoeck E. F., 1987, *ApJ*, 322, 412
 Burton M. G., Hollenbach D. J., Tielens A. G. G. M., 1990, *ApJ*, 365, 620B
 Burton M. G., Bulmer M., Moorhouse A., et al., 1992, *MNRAS*, 257, 1P
 Decin L., 2021, *ARA&A*, 59, 337D
 De Marco O., Akashi M., Akras S., et al., 2022, *NatA*, 6, 1421D
 Dyson J. E., Hartquist T. W., Redman M. P., et al., 2000, *Ap&SS*, 272, 197D
 Fang X., et al., 2018, *ApJ*, 859, 92
 García-Rojas J. et al., 2022, *MNRAS*, 510, 5444G
 Garcia-Segura et al. 2006, *ApJ*, 646L, 61G
 Gonçalves D. R., Corradi R. L. M., Mampaso A., 2001, *ApJ*, 547, 302G
 Gonçalves D. R. et al., 2009, *MNRAS*, 398, 2166G
 Graham J. R., et al., 1993, *ApJ*, 408L, 105G
 Kwitter K. B., Henry R. B. C., 2022, *PASP*, 134, 2001
 López J. A., Vázquez R., Rodríguez L. F., 1995, *ApJ*, 455, L63
 Manchado A., et al., 2015, *ApJ*, 808, 115M
 Mari M. B., Gonçalves D. R., Akras S., 2023a, *MNRAS*, 518, 3908M
 Mari M. B., Akras S., Gonçalves D. R., 2023b, *MNRAS*, 525, 1998M
 Marquez-Lugo R. A., Guerrero M. A., Ramos-Larios G., et al., 2015, *MNRAS*, 453, 1888M
 Matsuura, M., et al., 2009, *ApJ*, 700, 1067M
 Mellema G., et al., 1998, *A&A*, 331, 335M
 Monreal-Ibero A., Walsh J. R., 2020, *A&A*, 634A, 47M
 Perea-Calderón J. V., García-Hernández D. A., García-Lario P., et al., 2009, *A&A*, 495L, 5P
 Perinotto M., 2000, *Ap&SS*, 274, 205
 Ramstedt S., et al., 2020, *A&A*, 640A, 133R
 Reay et al. 1988, *MNRAS*, 232, 615R
 Redman M. P., Viti S., Cau P., Williams D. A., 2003, *MNRAS*, 345, 1291R
 Speck K. A., et al., 2002, *AJ*, 123, 346S

- Steffen W., López J. A. 2004, *ApJ*, 612, 319S
Sternberg A., Dalgarno A., 1989, *ApJ*, 338, 197S
Walsh J. R., et al., 2018, *A&A*, 620A, 169W
Weigelt G., et al. 2002, *A&A*, 392, 131W
Wesson R., Matsuura M., Zijlstra A. A., et al., 2023, arXiv230809027W
Woitke P., 2006, *A&A*, 452, 537W
Ziurys L. M., 2006, *PNAS*, 10312274Z